

Effect of FeO in the Slag and Silicon in the Metal on the Desulfurization of Hot Metal

P.K. IWAMASA and R.J. FRUEHAN

Work has been conducted to investigate the effects of FeO in the slag and silicon in the metal on hot metal desulfurization. Laboratory experimental results show that FeO decreases and silicon increases the rate of desulfurization. Silicon in the metal is consumed by the reduction of FeO and also by the desulfurization reaction. A mathematical kinetic model was developed to describe both the effects of silicon and FeO on desulfurization for the laboratory scale. The model predicts the sulfur and silicon content in the metal and the FeO and sulfur content in the slag as a function of time. It is based on four-component simultaneous mass transfer: sulfur and silicon in the metal and FeO and sulfur in the slag. Experimental results, the development of the kinetic model, and a comparison of the model and experimental results are presented.

I. INTRODUCTION

THE desulfurization of hot metal is a vital part of the steelmaking process since sulfur in many steel products is detrimental. In general, desulfurizing hot metal is more economical than desulfurizing steel, and about 90 pct of the metal produced in the iron blast furnace is desulfurized before it is sent to be processed in a steelmaking furnace. A common practice is the injection of a desulfurizing reagent through a lance. During injection, there are two sites at which sulfur is removed from the metal. Sulfur is removed by the reagent particles that are injected and rise in the metal bath and also by the slag that accumulates at the top of the metal. These reaction sites can be studied independently and are referred to as the transitory (rising particles) and the permanent contact (top slag) reactions. It has been shown that when the same amount of slag is either simply added to the top of the metal or injected, the sulfur content of the metal reaches the equilibrium amount at about the same time after the slag is introduced.^[1,2] The present study will focus only on the top slag reaction as results obtained from these findings can be used to predict the behavior during the injection desulfurization process. A subsequent publication will utilize the basis of the model presented here to demonstrate the effect of FeO in the slag and silicon in the metal on desulfurization in actual industrial practice.

Although hot metal desulfurization is a mature process, the effects of FeO in the slag have never been quantitatively assessed. The FeO present in the desulfurizing unit originates from two main sources. The first source is slag carried over from the iron blast furnace and the second is hot metal oxidized during tapping from the blast furnace and during transportation to the desulfurization station. The presence of FeO in the slag during desulfurization hinders both the thermodynamics and kinetics of the desulfurization process.

This can be demonstrated in the definition of the sulfur partition ratio, L_s , a measure of the thermodynamic ability of a slag to contain sulfur.^[3]

$$L_s = \frac{(\text{pct S})}{[\text{pct S}]} = \frac{f_s C_s}{h_o K_2} \quad [1]$$

where

(pct S) = weight percent of sulfur in the slag;

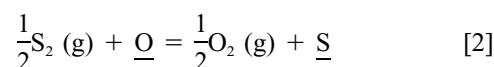
[pct S] = weight percent of sulfur in the metal;

f_s = activity coefficient of sulfur in metal relative to the 1 wt pct standard state;

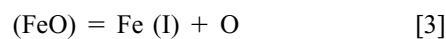
C_s = sulfide capacity of the slag (as defined by Richardson and Withers^[5]);

h_o = Oxygen potential of the system; and

K_2 = equilibrium constant for the slag and gas equilibrium:



FeO in the slag effects the sulfur partition ratio by controlling the oxygen potential at the interface between the slag and metal. This can be demonstrated by the chemical equilibrium between FeO in the slag and the liquid iron and the corresponding equilibrium constant expression:



$$K_3 = \frac{a_{\text{Fe}} h_o}{a_{\text{FeO}}^i} \quad [4]$$

where

a_{Fe} = activity of liquid iron; and

a_{FeO}^i = activity of FeO in the slag at the interface.

By substituting Eq. [4] into Eq. [1], it can be seen that the sulfur partition ratio is inversely proportional to the amount of FeO in the slag at the interface for a fixed value of C_s .

$$L_s \propto \frac{1}{(\text{pct FeO})_i} \quad [5]$$

As the amount of FeO in the slag at the interface increases, the thermodynamic ability of the slag to contain sulfur de-

P.K. IWAMASA, formerly Graduate Student, Department of Materials Science and Engineering, Carnegie Mellon University, is Research Associate, BHP Research, New South Wales 2287, Australia. R.J. FRUEHAN, Professor, is with the Department of Materials Science and Engineering, Carnegie Mellon University, Pittsburgh, PA 15213.

Manuscript submitted October 5, 1995.

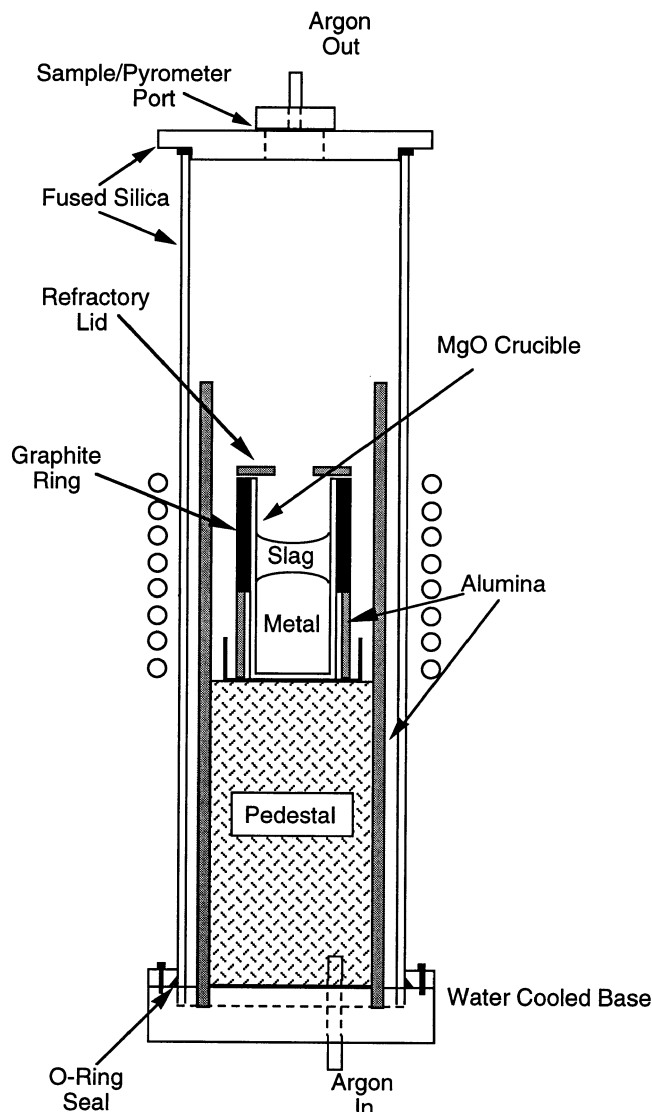
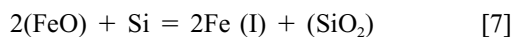
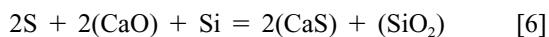


Fig. 1—Schematic of the experimental apparatus used for kinetic study.

creases for a fixed value of C_s . In reality, C_s may be a function of FeO and S content, but this effect is small.^[4]

The aim of this work is to determine the kinetics of desulfurization in the presence of silicon in the metal and simultaneous reduction of FeO from lime (CaO) based slags according to the following chemical reactions:



A mathematical kinetic model is also presented to describe the time dependence of the concentration of silicon and sulfur in the metal and FeO in the slag.

II. EXPERIMENTAL PROCEDURE

The experimental work included trials using 300 g of metal and 30 g of slag of the following chemistry.

Metal: carbon saturated
0.12, 0.45 pct Si

0.14 pct S
master slag:
(premelted) 50 pct CaO
45 pct SiO₂
5 pct MgO
slag addition: 0 to 5 pct FeO

Alloys, slags, and FeO used in the experiments carried out in this study were prepared as follows.

Master Alloys. An Inductotherm induction furnace was used to melt the metal alloys. Iron chips or lumps were placed in a graphite crucible and melted. Silicon in the form of ferro-silicon (50 pct Si) was added to the liquid metal and allowed to equilibrate for a few minutes. Sulfur was then added in the form of granular ferrous sulfide (FeS) and allowed to equilibrate for another few minutes. The metal was then cast into graphite crucibles (29-mm i.d., 50-mm o.d., and 305-mm height) and left to cool overnight. Once at room temperature, the resulting casting was cut, sandblasted, and ultrasonically cleaned to remove any surface residue.

Slag. One kilogram of the mixture of reagent grade powders (50 pct CaO, 45 pct SiO₂, 5 pct MgO) was mixed and placed in a high density MgO crucible (96-mm i.d., 102-mm o.d., and 152-mm height). The crucible was placed in a Lindberg molybdenum disilicide resistance box furnace and heated to a temperature of 1425 °C at a rate of 2 °C per minute. The furnace was stabilized at 1425 °C for 30 minutes, the slag and crucible were furnace cooled, and the slag was crushed.

FeO. FeO was prepared using a Lindberg silicon carbide resistance tube furnace. About 100 g of reagent grade Fe₂O₃ powder was placed in a steel crucible (39-mm i.d., 45-mm o.d., and 128-mm height) and placed in the reaction tube. The top was sealed and an alumina lance was placed through the lid to about 1 cm from the powder surface. A gas mixture of 50/50 CO/CO₂ was flowed through the lance at a rate of 2 cc/s. The furnace was heated to a temperature of 1150 °C and kept there for about 12 hours; it was then cooled to about 800 °C. The gas atmosphere was changed to argon for a 10-minute purge; then the cover of the furnace was opened and the crucible removed and quenched in a high flow rate of argon. X-ray diffraction analysis showed that the end product was converted (more than 99 pct) to FeO.

A. Kinetic Experiments

Experiments were run using a 10 kW Ameritherm induction furnace. A schematic of the apparatus is shown in Figure 1. The metal was placed in a magnesia crucible (inside diameter 32 mm) and gradually heated to 1450 °C. The experimental temperature was periodically measured with an optical pyrometer. The chamber was closed to the atmosphere and a low flow rate of argon (0.5 cc/s) was maintained within the furnace during the experiment. A graphite ring was used as a susceptor from the induction field to heat the slag layer over the metal. The slag was added by means of a funnel through the sample port, and metal and slag samples were taken at varying times from the time of slag addition. The metal samples were obtained using silica suction tubes and the slag samples with notched copper rods. The slag samples were chemically analyzed for FeO (total iron, assumed to be in the form of FeO) by

Table I. Starting Composition of Slag and Metal for Kinetic Experiments

Run Identification	[Pct S]	[Pct Si]	(Pct FeO)
S1	0.141	0.12	0.0
S2	0.143	0.12	5.0
S3	0.143	0.12	3.0
S4	0.143	0.12	1.0
S5	0.145	0.41	0.0
S6	0.144	0.43	5.0
S7	0.147	0.47	3.0
S8	0.147	0.44	1.0

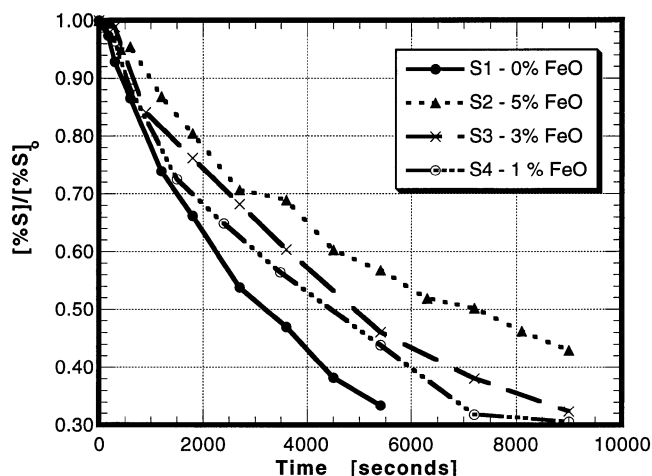


Fig. 2—Effect of FeO on desulfurization: experimental results for metal sulfur content as a function of time for initial slag FeO contents between 0 and 5 pct.

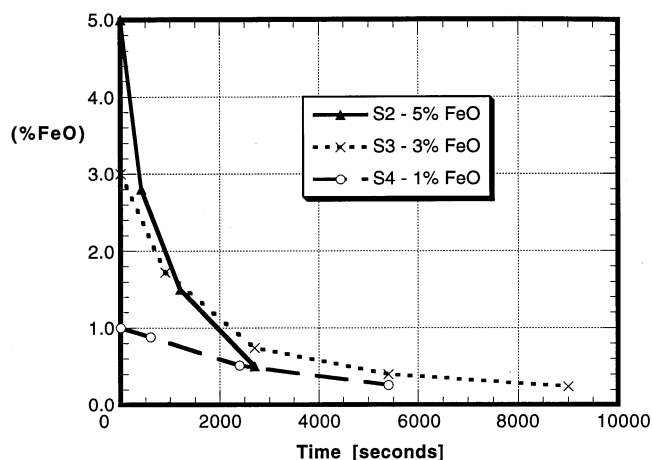


Fig. 3—FeO reduction: experimental results for slag FeO content as a function of time for initial slag FeO contents between 1 and 5 pct.

redox titration with $K_2Cr_2O_7$. The metal samples were analyzed for carbon and sulfur using a LECO* Analyzer pro-

*LECO is a trademark of LECO Corporation, St. Joseph, MI.

vided by the AISI Pilot Plant (Universal, PA). Silicon contents in the metal samples were determined using a wet chemical technique at Spectrochemical Laboratories (Pittsburgh, PA).

B. Constant Volume Pressure Increase Experiments

Experiments utilizing the constant volume pressure increase (CVPI) technique were carried out to investigate if there was any gas evolution between the slag and metal from experiments similar to those done in the induction furnace. The motivation for these experiments was to justify the mass transfer coefficients that were fit to the mathematical model. These experiments were also used to prove the assumption that the reduction of FeO in the slag by carbon dissolved in the metal producing carbon monoxide gas did not appreciably affect the mass balances used in the development of the mathematical model.

A Lindberg silicon carbide resistance furnace was used with a mullite reaction tube (48-mm i.d., 54-mm o.d., 610-mm length, and closed round at bottom). An alumina pedestal was placed at the bottom of the tube, and the MgO crucible containing the metal was seated on the pedestal. A mullite guiding tube (25-mm i.d., 32-mm o.d., and 457-mm length) cemented (AREMCO* Cermabond 503) to the

*AREMCO is a trademark of Aremco Products, Inc., Ossining, NY.

MgO crucible extended through the length of the furnace. The furnace was sealed and the temperature was slowly increased from room temperature to 1450 °C under an argon atmosphere. Once 1450 °C was obtained, the argon flow was stopped. Calibration of the equipment was carried out by injecting a known volume of air into the furnace and the response recorded by the data acquisition system. Once the calibration was completed, a port in the lid was opened and a pin sample was obtained. The slag was then added and the port quickly sealed. The exit port of the lid was connected to a pressure transducer (Daytronic 502) which was connected to an analog to digital converter and a data acquisition system. The data collected were in the form of volts vs time, and volts were converted to moles of gas using the calibration curve.

III. RESULTS

Table I outlines the starting composition of the slag and metal for the experiments carried out in this series. The normalized sulfur content of the metal as a function of time is shown in Figure 2 for experiments S1 through S4. These data clearly show the dependence of the desulfurization ability of a slag as a function of the amount of FeO added to the slag. In these experiments, the initial silicon content of the metal is 0.12 pct Si. As the initial amount of FeO in the slag increases, the desulfurization ability of the slag decreases as does the rate of sulfur removal. Figure 3 shows the concentration of FeO in the slag as a function of time. For the results presented here, the initial silicon (0.12 pct Si) and sulfur (0.14 pct S) contents were consistent. As seen from this plot, FeO is reduced out of the slag rather quickly and the equilibrium value for the concentration of FeO in the slag is quite low.

Figure 4 displays the time dependence of silicon concentration in the metal for the same series of experiments mentioned previously. As expected from the FeO reduction reaction and the results for FeO content in the slag, as the amount of FeO in the slag increases, more silicon is consumed. Silicon is stoichiometrically consumed in both the

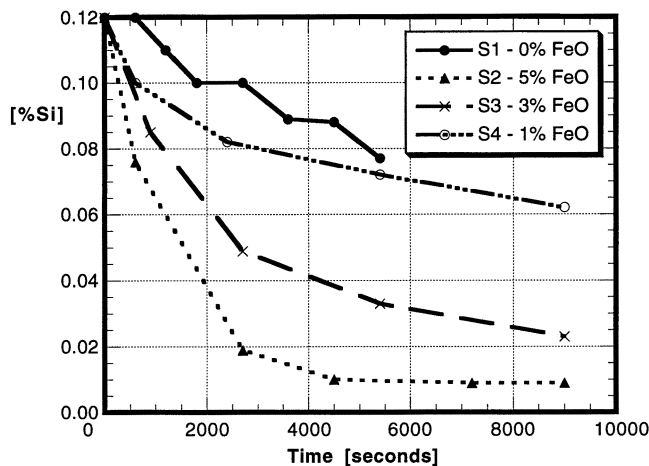


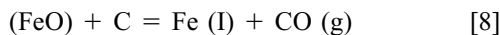
Fig. 4—Silicon removal during desulfurization: experimental results for metal silicon content as a function of time for initial slag FeO contents between 0 and 5 pct.

desulfurization reaction and the FeO reduction reaction. Mass balance calculations for silicon consumption for the series of experiments, where the initial silicon content in the metal is 0.12 pct, are presented in Table II. These calculations are based on the initial and final values of the constituents that were analyzed. As evident from the calculations presented in Table II, the mass balances between silicon in the metal are reasonable within a maximum 10 pct discrepancy. The contribution of silicon consumption from FeO and sulfur varies depending on the initial FeO content of the slag and is presented in Table III for the same series of experiments.

Figure 5 shows both the effects of FeO in the slag and silicon in the metal on desulfurization. A greater silicon content in the metal provides for better and more rapid sulfur removal for both cases where the slag contains 5 pct FeO and no FeO.

IV. MATHEMATICAL KINETIC MODEL

To better understand and analyze the results of the laboratory experiments, a kinetic model was developed. This section discusses the underlying assumptions that went into the development of the mathematical model based on chemical Reactions [6] and [7]. Sulfur, in the presence of silicon in the metal, is removed by a lime based reagent, and FeO in the slag is reduced by silicon in the metal. These assumptions will be shown to be consistent with the experimental results. The reduction of FeO in the slag by carbon in the metal, as presented in the following chemical reaction, is slow compared to the reaction between FeO and silicon.



Reaction [8] was neglected in the mathematical model, since it was determined to be relatively insignificant compared to Reactions [6] and [7]. Previous investigators have shown that Reaction [8] which involves three phases (metal, slag, and gas) proceeds at a relatively slow rate by means of gaseous intermediates.^[6,7,8] It was found that for a slag FeO content below about 2.5 pct, the rate is limited by the chemical reaction rate at the gas/metal interface. For

slags with higher FeO contents, the reaction is controlled by the kinetics of the chemical reaction at the slag/gas interface. Kinetics of chemical reactions involving two phases (slag and metal) are usually faster than three-phase reactions. Typical slag/metal reactions are mass transfer controlled in terms of elements diffusing through the slag and the metal with very fast chemical kinetics at the interface. The elimination of Reaction [8] in the mathematical model is further discussed in the results for the CVPI experiments.

A. Assessment of All Possible Rate Controlling Mechanisms

Before work on the model can commence, initial assumptions about the controlling mechanisms to the preceding reactions need to be made. There are many possible rate controlling steps that may influence the reaction and they are listed subsequently. It should be noted that compounds in the slag phase diffuse as ions. For example, the diffusing species for CaO are Ca^{2+} and O^{2-} ions. However, for charge neutrality, “CaO” can be considered as the equivalent diffusing compound.

- (1) Chemical reaction rate of Reference 6.
- (2) Chemical reaction rate of Reference 7.
- (3) Liquid-phase mass transfer of sulfur in the metal from the bulk metal to the interface between the slag and metal.
- (4) Liquid-phase mass transfer of silicon in the metal from the bulk metal to the interface between the slag and metal.
- (5) Liquid-phase mass transfer of CaO in the slag from the bulk slag to the interface between the slag and metal.
- (6) Liquid-phase mass transfer of “FeO” in the slag from the bulk slag to the interface between the slag and metal.
- (7) Liquid-phase mass transfer of iron in the metal from the interface between the slag and metal to the bulk metal phase.
- (8) Liquid-phase mass transfer of “ SiO_2 ” in the slag from the interface between the slag and metal to the bulk slag phase.
- (9) Liquid-phase mass transfer of “CaS” in the slag from the interface between the slag and metal to the bulk slag phase.

B. Elimination of Possible Rate Controlling Mechanisms

To a first approximation, the chemical rates were assumed to be fast, and the liquid phase mass transfers of lime and silica in the slag are also assumed to be fast since the slag composition is rich in both lime and silica which results in a high driving force for mass transfer. As a parallel argument, liquid-phase mass transfer of iron in the metal phase is taken to be fast. After elimination of the previous mechanisms, the remaining possible rate controlling phenomena are the following:

- (1) liquid-phase mass transfer of sulfur in the metal;
- (2) liquid-phase mass transfer of silicon in the metal;
- (3) liquid-phase mass transfer of “FeO” in the slag; and
- (4) liquid-phase mass transfer of “CaS” or, more simply, sulfur (S^{2-}) in the slag.

Table II. Mass Balance Calculations for Experiments S1 through S4

Run Identification	Initial FeO Content in the Slag (Wt Pct)	Moles Silicon Consumed (n_{Si})	Moles FeO Reduced (n_{FeO})	Moles Sulfur Lost (n_S)	$0.5 n_{FeO} + 0.5 n_S$	Difference between (n_{Si}) and ($0.5 n_{FeO} + 0.5 n_S$)
S1	0	0.00471	0	0.00903	0.00452	+ 5 pct
S2	5	0.01210	0.01920	0.00784	0.01350	- 10 pct
S3	3	0.01080	0.01200	0.00943	0.01070	+ 1 pct
S4	1	0.00634	0.00316	0.00948	0.00632	+ 0.3 pct

Table III. Relative Contribution to Silicon Consumption for Experiments S1 through S4

Run Identification	Initial FeO Content in the Slag (Wt Pct)	Pct Silicon Consumed by FeO Reduction	Pct Silicon Consumed by Desulfurization
S1	0	0	100
S2	5	71	29
S3	3	56	44
S4	1	25	75

The model is based upon the four mechanisms presented earlier, and because the reactions are mass transfer controlled, the flux of these elements and species at any given time during the process can be defined as follows:

$$J_S^m = m_S^m (C_S^m - C_S^{m,i}) \quad [9]$$

$$J_{Si}^m = m_{Si}^m (C_{Si}^m - C_{Si}^{m,i}) \quad [10]$$

$$J_{FeO}^S = m_{FeO}^S (C_{FeO}^S - C_{FeO}^{S,i}) \quad [11]$$

$$J_S^S = m_S^S (C_S^S - C_S^{S,i}) \quad [12]$$

where

J_A^b = flux of A in phase (slag or metal) b (moles $cm^{-2} s^{-1}$);

m_A^b = mass transfer coefficient of A in phase b ($cm s^{-1}$);

C_A^b = concentration of A in bulk b phase (moles cm^{-3}); and

$C_A^{b,i}$ = concentration of A in the b phase at the interface between the slag and metal (moles cm^{-3}).

C. Sulfur Mass Transfer

The mass transfer behavior of sulfur is well known and has been extensively studied. It has been found that, in general, it is the simultaneous mass transfer of sulfur in the metal and sulfur in the slag that controls sulfur removal from metal. This is represented by equating the sulfur fluxes ($J_S^m = J_S^S$) and is schematically displayed in Figure 6(a).

$$m_S^m (C_S^m - C_S^{m,i}) = m_S^S (C_S^{S,i} - C_S^S) \quad [13]$$

In Eq. [13], the surface concentrations of sulfur in the slag and metal are related to each other by the sulfur partition ratio. In the model, the concentration of sulfur in the slag and metal are continually changing and the sulfur partition ratio is defined at each time-step. The mass transfer of sulfur in the metal phase can be rewritten to include the mass

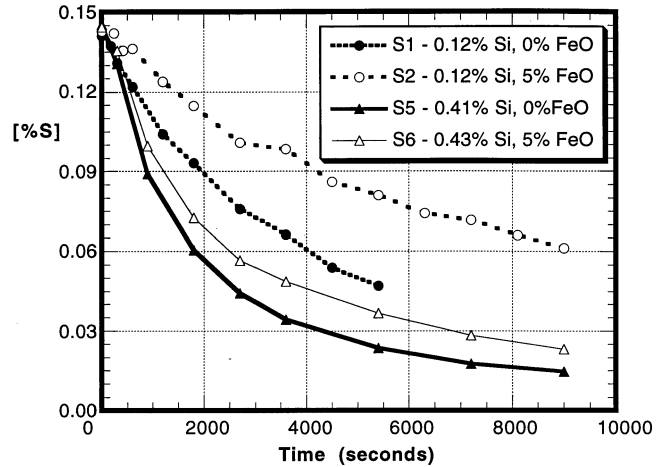


Fig. 5—Effect of FeO and silicon on desulfurization: experimental results for metal sulfur content as a function of time for initial slag FeO contents of 0 and 5 pct and initial silicon contents of 0.12 and 0.41/0.43 pct Si.

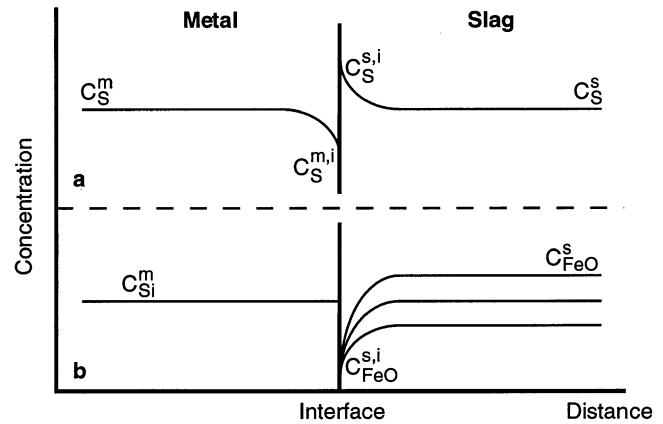


Fig. 6—Schematic concentration profile of elements in the slag and metal phases near the interface: (a) sulfur in the metal and slag; and (b) silicon in the metal and FeO in the slag based on mass transfer of FeO in the slag.

transfer of sulfur in the slag phase:

$$J_S^m = m_0 \left(C_S^m - \frac{C_S^S \rho_m}{L_S \rho_s} \right) \quad [14]$$

where

ρ_m = density of metal ($g cm^{-3}$);

ρ_s = density of slag ($g cm^{-3}$);

m_0 = time-dependent overall mass-transfer coefficient for sulfur in the metal:

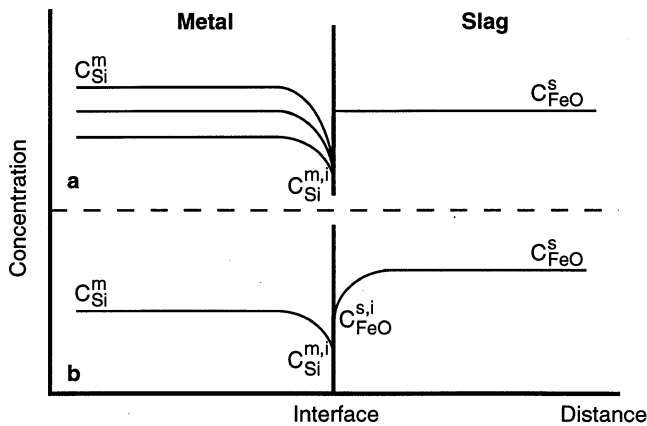


Fig. 7—Schematic concentration profile of elements in the slag and metal phases near the interface: (a) silicon in the metal and FeO in the slag based on mass transfer of silicon in the metal; and (b) silicon in the metal and FeO in the slag based on simultaneous mass transfer of FeO in the slag and silicon in the metal.

$$m_0 = \frac{\left(\frac{m_S^m m_S^s L_S \rho_s}{\rho_m} \right)}{\left(\frac{m_S^s L_S \rho_s}{\rho_m} + m_S^m \right)} \quad [15]$$

For most desulfurizing slags (for instance, lime-rich slags), the sulfur partition ratio L_S is quite large, on the order of 10^2 to 10^4 . In those limiting cases, the overall mass transfer coefficient for sulfur (m_0) will reduce simply to the mass transfer coefficient for sulfur in the metal (m_S^m). Since FeO in the slag was being reduced and silicon in the metal was being oxidized, the concentration gradient of FeO and silicon would affect the interfacial conditions for sulfur transfer. Therefore, the coupled sulfur mass transfers in the slag and metal were ruled out as the only two rate controlling mechanisms.

D. Mass Transfer of FeO in the Slag

The mass transfer of FeO from the bulk slag to the interface between the slag and metal was the next mechanism considered. Because of the ionic nature of the slag, a more accurate description of FeO transfer is the mass transfer of Fe^{2+} and O^{2-} ions. Since mass transfer will depend on the slower of the two ions, namely, O^{2-} , it should be an acceptable assumption to consider the mass transfer of the compound itself. A simplified way to conceptualize FeO transfer is to look at a schematic of the concentration profiles of FeO in the slag and silicon in the metal, as shown in Figure 6(b).

If the rate is controlled only by mass transfer of FeO in the slag, the driving force for FeO reduction is proportional to the difference between the concentration of FeO in the bulk slag and the concentration of FeO at the interface ($C_{\text{FeO}}^s - C_{\text{FeO}}^{s,i}$). The concentration of FeO at the interface is in equilibrium with the silicon in the metal. This means that for a constant silicon content, $C_{\text{FeO}}^{s,i}$ is a low, constant value and is independent of the bulk FeO concentration. The oxygen potential at the interface is defined by the equilibrium between FeO at the interface and the iron in the metal. Also, the sulfur partition ratio is inversely proportional to

the interfacial concentration of FeO. The sulfur partition ratio would then be a constant value, independent of the FeO content of the bulk slag. Based on the results of the experiments, desulfurization behavior was dependent on the bulk FeO content in the slag so mass transfer of FeO in the slag was ruled out as the sole rate controlling step.

E. Mass Transfer of Silicon in the Metal

The mass transfer of silicon from the bulk slag to the interface between the slag and metal is examined next. This is shown schematically in Figure 7(a). If the mass transfer of silicon in the metal is the sole rate controlling step, the driving force for silicon oxidation is proportional to the difference between the bulk and interfacial concentration of silicon in the metal, ($C_{\text{Si}}^m - C_{\text{Si}}^{m,i}$). The concentration of silicon at the interface is a low and constant value and sets the oxygen potential for desulfurization. In this case, the sulfur partition ratio is inversely proportional to the interfacial concentration of silicon which is set by the equilibrium between the slag and the metal at the interface and independent of the silicon content of the bulk metal. Based on the experimental results, desulfurization is dependent on the bulk silicon content of the metal, and mass transfer of silicon in the metal is ruled out as the sole rate controlling step.

F. Model Basis: Flux Equations

Sulfur transfer in the metal and slag, mass transfer of FeO in the slag, and mass transfer of silicon in the metal considered separately were eliminated as the individual rate controlling steps for the reactions kinetics. Therefore, the model is developed utilizing dynamic simultaneous mass transfer of sulfur in the slag, sulfur in the metal, silicon in the metal, and FeO in the slag. Based on the stoichiometry for chemical Reactions [6] and [7], the balance of the mass fluxes between silicon in the metal with FeO in the slag and sulfur in the metal at any time during the process is represented as

$$2 J_{\text{Si}}^m = J_{\text{FeO}}^s + J_{\text{S}}^m \quad [16]$$

A schematic of the overall process of combined FeO and silicon diffusion is shown in Figure 7(b).

These assumptions do not provide for *a priori* knowledge of the dependency of the sulfur partition ratio, since the interfacial concentrations of silicon in the metal and FeO in the slag are in equilibrium and are no way related to the bulk concentrations. The interfacial concentrations of silicon in the metal and FeO in the slag are related by the equilibrium constant for chemical Reaction [7]. Therefore, the mathematical model is based on the preceding flux equations and the sulfur balance Eq. [14], which are solved simultaneously at each time-step.

G. Mass Transfer Coefficients

Since the experiments were inductively stirred, the mass transfer coefficient for sulfur and FeO in the slag and sulfur and silicon in the metal can be related to one another based on the relationship presented by Higbie.^[9]

$$m = \left(\frac{4Dv}{\pi r} \right)^{1/2} \quad [17]$$

Table IV. Diffusion Data for Sulfur and Silicon in Carbon Saturated Iron at 1450 °C

Diffusing Element	Concentration (Wt Pct)	D (cm ² /s)	Reference
S	<0.64	3.13×10^{-5}	10
S	—	3.09×10^{-5}	11
Si	—	2.20×10^{-5}	11

Table V. Diffusion Data for Sulfur and Oxygen in Slags at 1450 °C

Diffusing Element	Slag Composition (Wt Pct)	D (cm ² /s)	Reference
O ^[17]	40CaO	6.17×10^{-6}	12
	40SiO ₂		
	20Al ₂ O ₃		
O ^[18]	40CaO	7.76×10^{-6}	12
	40SiO ₂		
	20Al ₂ O ₃		
O	38CaO	7.5×10^{-6}	13
	42SiO ₂		
	20Al ₂ O ₃		
S	50.6CaO	7.13×10^{-7}	14
	39SiO ₂		
	10.4Al ₂ O ₃		
S	40.8CaO	6.65×10^{-7}	15
	40.8SiO ₂		
	51Al ₂ O ₃		
	3FeO 0.4S		

where

m = mass transfer coefficient (cm s⁻¹);
 D = diffusivity (cm² s⁻¹);
 v = surface velocity (cm s⁻¹); and
 r = radius of the crucible (cm).

Diffusion data for sulfur and silicon in carbon saturated iron and relevant components in example slags as presented in the literature are summarized in Tables IV and V. Based on average values obtained for the diffusivity of sulfur and silicon in the metal as presented in Table IV and the ratios of the square roots of the diffusivities, the relationship between the mass transfer for the elements in the metal phase was taken to be

$$m_S^m = 1.2 m_{Si}^m \quad [18]$$

Likewise for the slag phases, the following relationship was made based on the data presented in Table V:

$$m_S^s = 0.31 m_{FeO}^s \quad [19]$$

In the model, the values used for m_{Si}^m and m_{FeO}^s were determined from the experimental data and were not derived from first principles. The values for m_S^m and m_S^s were calculated from the input values for m_{Si}^m and m_{FeO}^s by Eqs. [18] and [19]. Therefore, the model only has two adjustable mass transfer parameters, one for the slag and one for the metal.

H. Governing Flux Equation

The governing dynamic mass transfer flux equation, an expansion of Eq. [16], is represented as follows:

$$2 m_{Si}^m (C_{Si}^m - C_{Si}^{m,i}) = m_{FeO}^s (C_{FeO}^s - C_{FeO}^{s,i}) + m_0 (C_S^m - \frac{C_S^s \rho_m}{L_s \rho_s}) \quad [20]$$

Equation [20] is based on Eq. [16], which assumes silicon is consumed by FeO reduction and the desulfurization reaction.

I. Interfacial Concentration of FeO in the Slag

The interfacial concentration of FeO in the slag is defined in terms of the interfacial concentration of silicon in the metal using the equilibrium constant for chemical Reaction [7] and is solved at each time-step.

$$K_7 = \frac{a_{Fe}^2 a_{SiO_2}}{f_{Si}^i [\text{pct Si}]^i \gamma_{FeO}^2 (\text{pct FeO})^{i,2}} \left(\frac{100 n_s MW_{FeO}}{W_s} \right)^2 \quad [21]$$

where

a_{Fe} = activity of liquid iron;
 a_{SiO_2} = activity of silica in the slag;
 f_{Si}^i = activity coefficient of silicon in the metal at the slag/metal interface with respect to the 1 wt pct standard state;
 $[\text{pct Si}]^i$ = interfacial silicon concentration in the metal (wt pct);
 $(\text{pct FeO})^i$ = interfacial FeO concentration in the slag (wt pct);
 γ_{FeO} = activity coefficient for FeO in the slag
 W_s = slag weight (g); and
 n_s = number of moles in the slag.

The interfacial concentration of FeO in the slag can be expressed as

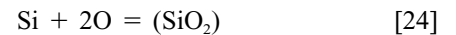
$$(\text{pct FeO})^i = G_{FeO} \left(\frac{1}{[\text{pct Si}]^i} \right)^{1/2} \quad [22]$$

where

$$G_{FeO} = \left(\frac{a_{Fe}^2 a_{SiO_2}}{f_{Si}^i \gamma_{FeO}^2 K_7} \right)^{1/2} \left(\frac{100 n_s MW_{FeO}}{W_s} \right) \quad [23]$$

J. Oxygen Potential at the Slag Metal Interface

The interfacial oxygen potential is defined by the time-dependent equilibrium between silica in the slag and silicon in the metal. Because of the interfacial equilibrium conditions between the constituents in chemical Reaction [7], the oxygen potential defined by the equilibrium between silica in the slag and silicon in the metal will be identical to the oxygen potential defined by FeO in the slag and the liquid iron. Therefore, the following reaction is at equilibrium at the slag/metal interface:



The equilibrium constant of this reaction is

$$K_{24} = \frac{a_{SiO_2}}{f_{Si}^i [\text{pct Si}]^i (h_o)^2} \quad [25]$$

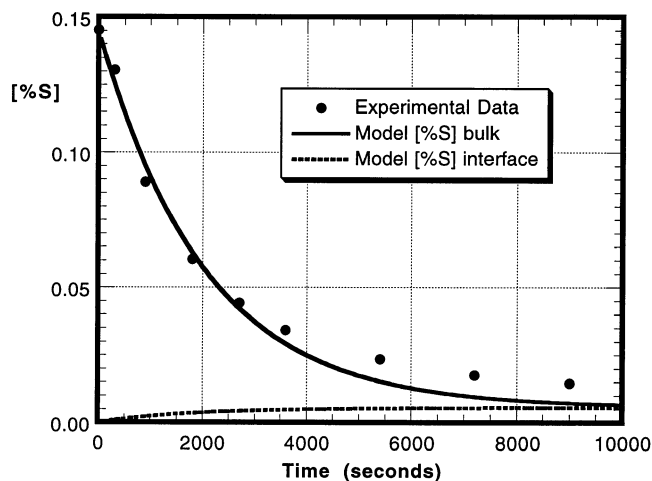


Fig. 8—Experimental data and model results for metal sulfur contents as a function of time for experiment S5. Initial experimental conditions: 0.145 [pct S], 0.41 [pct Si], and 0 (pct FeO).

The oxygen potential at the slag/metal interface is defined by

$$h_{\text{O}} = \left(\frac{f_{\text{Si}}^i [\text{pct Si}]^i K_{24}}{a_{\text{SiO}_2}} \right)^{1/2} \quad [26]$$

K. Sulfide Capacity of the Slag

Besides the oxygen potential of the system, the sulfide capacity of the slag, C_s , must be known to calculate the sulfur partition ratio. In this model, the sulfide capacity used is taken from the data originally generated by Kalyanram *et al.* for a slag of similar composition to the one used in the experiments.^[16] Kalyanram *et al.* made measurements at 1500 °C, so a temperature correction for the temperature of the experiments used in this study (1450 °C) was taken from work carried out by Nassaralla *et al.*^[17] The value used for the sulfide capacity in this study was 9.33×10^{-4} , which was found to be consistent with the average sulfide capacities computed from the final experimental values for the experiments that were assumed to reach equilibrium.

For example, in experiment S6, the sulfur partition ratio calculated by mass balance of sulfur at the end of the experiment was $L_s = 52.6$. The final FeO content in the slag equaled 0.13 pct FeO. The oxygen potential was based on the final FeO content in the slag and the activity of liquid iron in the metal. Based on Eq. [1], the sulfide capacity was determined to be 9.4×10^{-4} . The value used for C_s was taken to be constant for the duration of the experiment since the bulk slag composition did not appreciably change. For the model, the sulfur partition ratio was calculated (Eq. [1]) based on the oxygen potential of the system and the sulfide capacity of the slag, and the sulfur flux equation was solved.

L. Interfacial Concentration of Silicon in the Metal

The overall flux equation which is solved at each time-step is recast in terms of the interfacial concentration of silicon in the metal:

$$[\text{pct Si}]^i = [\text{pct Si}] - \left(\frac{m_{\text{FeO}}^s \rho_s}{MW_{\text{FeO}}} \right) \left(\frac{MW_{\text{Si}}}{2 m_{\text{Si}}^m \rho_m} \right) \left((\text{pct FeO}) - G_{\text{FeO}} \left(\frac{1}{[\text{pct Si}]^i} \right)^{1/2} \right) - \left(\frac{m_0 \rho_m}{MW_s} \right) \left(\frac{MW_{\text{Si}}}{2 m_{\text{Si}}^m \rho_m} \right) \left([\text{pct Si}] - \frac{(\text{pct S})}{L_s} \right) \quad [27]$$

As presented in Eq. [27], $[\text{pct Si}]^i$ is not a simple algebraic expression and is solved by a numeric iteration technique. The interfacial silicon content in the metal is solved and is used as the basis for solving for the interfacial concentrations of the FeO in the slag. These values are solved at each time-step and then the flux equations^[9–12] are solved.

A computer program was written in THINK Pascal for the MACINTOSH* for this kinetic model. In this program,

*MACINTOSH is a trademark of Apple Computers, Inc., Cupertino, CA.

the process variables of the system are read as input (temperature, slag and metal weight, and composition). The only other input variables in the program are the mass transfer parameters for FeO in the slag and silicon in the metal. The program output consists of the following bulk and interfacial concentrations as a function of time: sulfur in slag, sulfur in the metal, FeO in slag, and silicon in metal.

V. DISCUSSION

A. Kinetic Experiments

The mathematical model developed was utilized to analyze the results of the small scale experiments. In this analysis, the model is fit to the experimental results by obtaining the “best-fit” values for the mass transfer coefficients (m_{Si}^m and m_{FeO}^s). The mass transfer coefficients used in the model which best fit the experimental data are

$$\begin{aligned} m_{\text{Si}}^m &= 0.003 \text{ cm s}^{-1} \\ m_{\text{FeO}}^s &= 0.002 \text{ cm s}^{-1} \end{aligned}$$

In experiments carried out in similar types of induction furnaces, the mass transfer coefficient is normally somewhat larger than was observed in this study. This may be due to the graphite ring consuming the bulk of the induction coupling and the surface velocity at the interface between the slag and metal not being as high as in the previous work where no graphite ring was used. The importance of the surface velocity at the slag/metal interface to determine the mass transfer coefficient in an inductively stirred melt was presented in Eq. [17]. Another contribution to this low mass transfer coefficient as related to the velocity at the interface of the slag and metal is the resistance that the slag provides for flow. Also, it would be expected from the diffusivity data that the value of m_{FeO}^s would be about half of m_{Si}^m , and this is about what was observed. Actually, m_{FeO}^s was greater than half of m_{Si}^m , and this could be attributed to the evolution of gas at the interface between the slag and the metal. This is discussed later in detail.

Figures 8 and 9 display the experimental results and the kinetic model output for the sulfur and silicon contents in the metal for experiment S5, where no FeO was added to the slag. Since there was no FeO present in the slag, only the desulfurization reaction (chemical Reaction [6]) was

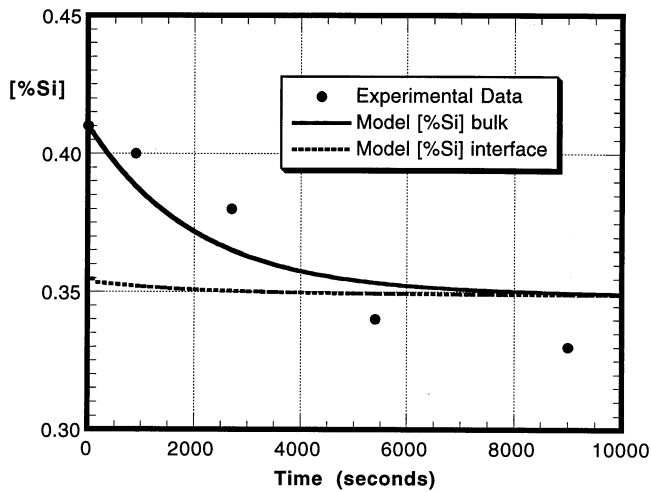


Fig. 9—Experimental data and model results for metal silicon content as a function of time for experiment S5. Initial experimental conditions: 0.145 [pct S], 0.41 [pct Si], and 0 (pct FeO).

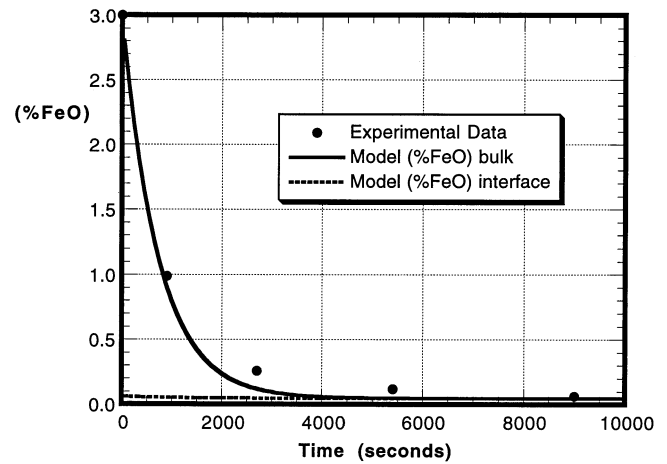


Fig. 12—Experimental data and model results for slag FeO content as a function of time for experiment S7. Initial experimental conditions: 0.147 [pct S], 0.47 [pct Si], and 3 (pct FeO).

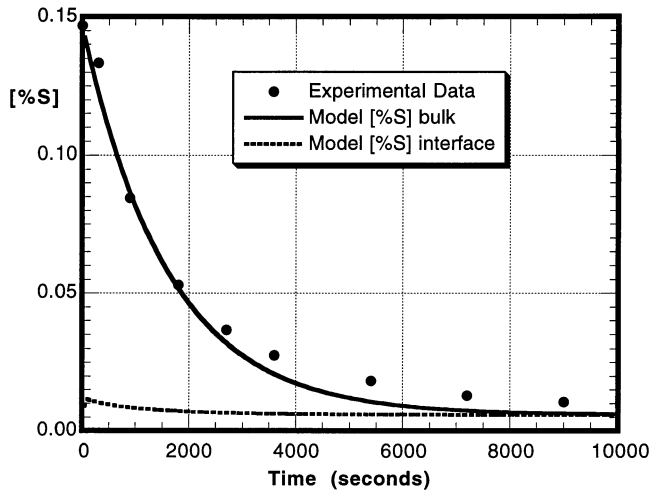


Fig. 10—Experimental data and model results for metal sulfur content as a function of time for experiment S7. Initial experimental conditions: 0.147 [pct S], 0.47 [pct Si], and 3 (pct FeO).

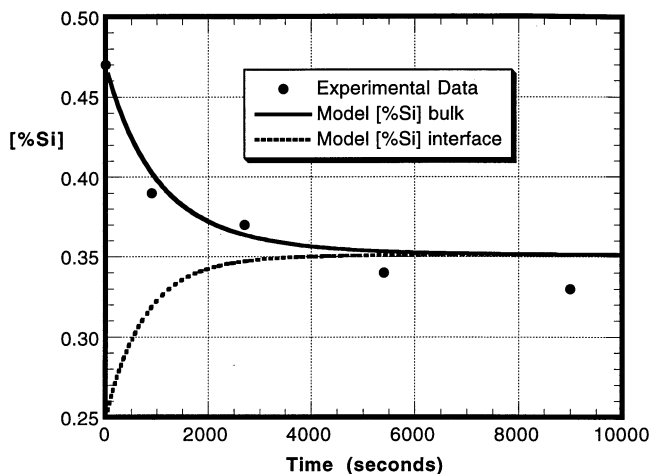


Fig. 11—Experimental data and model results for metal silicon content as a function of time for experiment S7. Initial experimental conditions: 0.147 [pct S], 0.47 [pct Si], and 3 (pct FeO).

considered in this case, where the moles of silicon lost from the metal is twice the moles of sulfur lost from the metal.

The agreement between the experimental data and the model results is quite good for the sulfur profile but not as good for the silicon. As seen from these figures, the interfacial (equilibrium) concentrations of sulfur and silicon are plotted along with their respective bulk concentrations. It can be seen that as the reaction proceeds, the bulk concentrations tend to the equilibrium concentrations, as expected. There is a reasonable fit of the experimental results with the calculated values obtained from the mathematical model. Since this simplified case utilizes both the metal and slag mass transfer coefficients, it can be assumed that the values used for m_s^m and m_s^s are reasonable and should be used in the case where FeO is present in the slag. In the experiments where FeO is present in the slag, it is difficult to compare the model results with the experimental data since the starting amount of FeO in the slag is not known accurately. Experimentally, the FeO powder is added to the master slag when it is at room temperature and mechanically mixed. This “cold” slag is then introduced to the metal melt which is at 1450 °C, and the starting time for the desulfurization of the metal is defined as this point. The problem inherent in this method is the fact that the slag does not melt instantaneously as assumed. From visual inspection of the procession of the experiments, it takes a few minutes for the slag to melt and cover the metal surface.

Figures 10 through 12 display the experimental data and model predictions for the results of experiment S7, where the initial cold amount of FeO in the slag is 3 pct and the initial silicon content in the metal is 0.47 pct. Figure 10 shows the amount of sulfur in the metal as a function of time as compared to the bulk concentration predicted from the model. Also, the interfacial concentration of sulfur in the metal is shown in this plot. Figure 11 displays the silicon content in the metal vs time, and Figure 12 shows the amount of FeO in the slag vs time. The model was run with the initial amount of FeO in the slag as 3 pct. The plots display that equilibrium is obtained near the end of the experiment, about 8000 seconds after the slag is added to the melt, when the bulk concentration profiles and interfacial concentration profiles merge. The experimental data

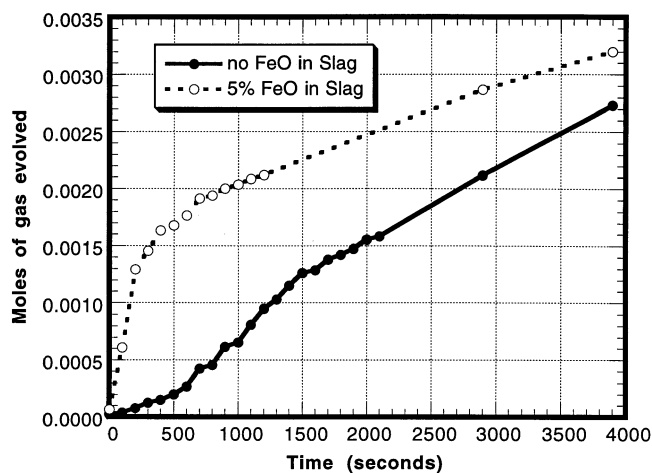


Fig. 13—Experimental results for CVPI experiments comparing the moles of gas evolved for experiments where there was 0 or 5 pct FeO in the slag.

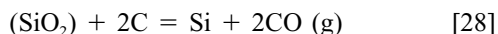
and the model predictions fit reasonably well. Similar agreement between the experimental results and model predictions were obtained with the other slag FeO contents and metal silicon contents.

Based on the experimental data and the results obtained from the model, the basis of the mathematical model seems to be viable. The presence of FeO in the slag does affect desulfurization of hot metal, and as the amount of FeO in the slag increases, the desulfurization rate decreases and the equilibrium sulfur content in the metal increases. Silicon in the metal is stoichiometrically consumed by two reactions: the desulfurization reaction and reduction of FeO from the slag.

B. CVPI Experiments

Experiments were carried out to investigate if there was any evolution of gas from reactions between the slag and metal for the kinetic experiments. Based on the diffusivity data presented, it is expected that the mass transfer coefficients for elements in the slag phase should be about half of those in the metal phase for the case where there is a stagnant slag metal interface. (The diffusivity of oxygen in the slag is about a factor of 4 less than the diffusivity of silicon in the metal, and they are related by the square root of the diffusivity). Since it was found that the mass transfer coefficients for the slag used in the kinetic model were comparatively greater than expected, it was proposed that there may be some evolution of gas at the interface between the slag and metal that would increase the mixing in the slag phase and promote better mass transfer kinetics.

Results from these experiments with 0 and 5 pct FeO in the slag are presented in Figure 13 for metal initially containing 0.17 pct silicon and 0.19 pct sulfur. The results show that there is some gas evolution during the experiments. It may be surprising that gas is produced in the experiments, where FeO is not present in the slag, but it has been found that the following chemical reaction may take place at the slag/metal interface:^{17]}



Exit gas from some of these experiments was analyzed using a mass spectrometer (Dycor M100 Quadrupole Gas Analyzer), and it was found that the gas that evolved was primarily CO with some CO₂. The balance of the gas produced in the experiments where FeO was present in the slag was assumed to be from the chemical reaction mentioned previously.

This amount of gas evolved was assumed to be enough to provide for an increased mass transfer over the stagnant case, but not a significant amount to account for it in the mass balances for the model. The total amount of FeO that is consumed by carbon in the metal (the difference of these two plots) is determined to be about 5 pct of the total amount of FeO in the slag that is reduced. This would signify that the bulk (95 pct) of the FeO is reduced by silicon in the metal and would not significantly alter the mass balances assumed in the model.

For the experiment where no FeO was present in the slag, about 0.0027 moles of CO (g) were produced throughout the duration of the experiment. This amount of gas corresponds to 0.00135 moles of silica that are reduced (Eq. [28]), which equals about 7 pct of the total initial silicon content in the metal. Therefore, the amount of silicon in the metal available for desulfurization may actually be a little higher than expected. There may also be experimental reasons for measuring an increase in pressure in these experiments that are independent of any reaction between the slag and metal. These reasons include the initial heating and melting of the slag and shifting of the reaction tube as it was sealed. Like carbon reduction of FeO, it was assumed that this 7 pct increase in the silicon content was insignificant in the model mass balances.

A subsequent publication will include a scale up and expansion of this kinetic model to include desulfurization as pertaining to the AISI Direct Steelmaking process. Also, submerged injection of the desulfurizer will be incorporated in the model to describe the industrial hot metal desulfurization process.

VI. CONCLUSIONS

Experiments with carbon saturated iron containing silicon and sulfur and a slag of nominal composition 50 pct CaO, 45 pct SiO₂, and 5 pct MgO, with additions of FeO, were carried out in this study. A mathematical kinetic model was developed to predict sulfur, silicon, and FeO transfer to describe the results of the laboratory experiments. The results from the laboratory experiments and the model show the following.

1. As FeO in the slag decreases, the desulfurization rate increases and the final sulfur equilibrium content in the metal is lowered. The oxygen potential at the interface between the slag and metal is lower with lower FeO contents in the slag, which increases the sulfur partition ratio.
2. Greater desulfurization results as the amount of silicon in the metal is increased. Higher contents of silicon in the metal provide for a lower equilibrium FeO content in the slag at the slag metal interface and a greater driving force for FeO reduction from the slag. This also increases the sulfur partition ratio of the slag.

The kinetic model that was developed accurately predicted the sulfur and silicon contents in the metal and FeO contents in the slag. This model was based on four-component mass transfer: sulfur and silicon in the metal and FeO and sulfur in the slag. It requires two adjustable parameters, the mass transfer coefficient of silicon in the metal and FeO in the slag. The mass transfer coefficients of sulfur in the metal and slag are related to those of silicon in the metal and FeO in the slag by the ratio of the square roots of the diffusivities. The model describes sulfur removal from the metal, silicon oxidation from the metal, and FeO reduction out of the slag. Furthermore, the mass transfer coefficients used in the model are reasonable, considering the diffusivities of the elements and fluid flow condition of the laboratory experiments.

REFERENCES

1. S. Ohguchi and D.G.C. Robertson: *Ironmaking and Steelmaking*, 1984, vol. 11 (5), pp. 262-73.
2. W.H. VanNiekerk: Ph.D. Thesis, University of Pretoria, Pretoria, Republic of South Africa, 1991.
3. A.H. Chan and R.J. Fruehan: *Metall. Trans. B*, 1986, vol. 17B, pp. 491-96.
4. R.G. Reddy and M. Blander: *Metall. Trans. B*, 1987, vol. 18B, pp. 591-96.
5. F.D. Richardson and G. Withers: *J. Iron Steel Inst*, 1950, pp. 66-71.
6. I.D. Sommerville, P. Grieveson, and J. Taylor: *Ironmaking and Steelmaking*, 1980, vol. 7 (1), pp. 25-32.
7. K. Upadhy, I.D. Sommerville, and P. Grieveson: *Ironmaking and Steelmaking*, 1980, vol. 7 (1), pp. 33-36.
8. D.J. Min and R.J. Fruehan: *Metall. Trans. B*, 1992, vol. 23B, pp. 29-37.
9. R. Higbie: *Am. Inst. Chem. Eng.*, 1935, pp. 365-89.
10. L. Yang and G. Derge: *Metallurgical Society Conf., vol. 7, Physical Chemistry of Process Metallurgy, Part 1*, AIME, Pittsburgh, PA, 1959, G.R. St. Pierre, ed., Interscience Publishers, New York, 1961, pp. 503-21.
11. T. Saito, Y. Kawai, K. Maruya, and M. Maki: *Metallurgical Society Conf., Vol. 7: Physical Chemistry of Process Metallurgy, Part 1*, AIME, Pittsburgh, PA, 1959, G.R. St. Pierre, ed., Interscience Publishers, New York, 1961, pp. 523-33.
12. P.J. Koros and T.B. King: *Trans. TMS-AIME*, 1962, vol. 224, pp. 299-306.
13. R.F. Johnson, R.A. Stark, and J. Taylor: *Ironmaking and Steelmaking*, 1974, No. 4, pp. 220-27.
14. *Handbook of Physico-Chemical Properties at High Temperature*, Y. Kawai and Y. Shiraishi, eds., Iron and Steel Institute of Japan, Tokyo, 1988.
15. B. Ozturk, R. Roth, and R.J. Fruehan: *Iron Steel Inst. Jpn. Int.*, 1994, vol. 3 (8), pp. 663-69.
16. M.R. Kalyanram, T.G. Macfarlane, and H.B. Bell: *J. Iron Steel Inst.*, 1960, May, pp. 58-64.
17. C.L. Nassaralla, B. Sarma, A.T. Morales, and J.C. Meyers: *Proc. Ethem T. Turkdogan Symp.*, Iron and Steel Society, Pittsburgh, PA, 1994, pp. 61-71.